

# Probabilistic Hierarchical Forecasting with Deep Poisson Mixtures

Kin G. Olivares<sup>a</sup>, O. Nganba Meetei<sup>b</sup>, Ruijun Ma<sup>b</sup>, Rohan Reddy<sup>b</sup>,  
Mengfei Cao<sup>b</sup>, Lee Dicker<sup>b</sup>

<sup>a</sup>*Auton Lab, School of Computer Science, Carnegie Mellon University, Pittsburgh, PA*

<sup>b</sup>*Forecasting Science, Amazon, New York, NY*

---

## Abstract

Hierarchical forecasting problems arise when time series have a natural group structure, and predictions at multiple levels of aggregation and disaggregation across the groups are needed. In such problems, it is often desired to satisfy the aggregation constraints in a given hierarchy, referred to as hierarchical coherence in the literature. Maintaining hierarchical coherence while producing accurate forecasts can be a challenging problem, especially in the case of probabilistic forecasting. We present a novel method capable of accurate and coherent probabilistic forecasts for hierarchical time series. We call it Deep Poisson Mixture Network (DPMN). It relies on the combination of neural networks and a statistical model for the joint distribution of the hierarchical multivariate time series structure. By construction, the model guarantees hierarchical coherence and provides simple rules for aggregation and disaggregation of the predictive distributions. We perform an extensive empirical evaluation comparing the DPMN to other state-of-the-art methods which produce hierarchically coherent probabilistic forecasts on multiple public datasets. Compared to existing coherent probabilistic models, we obtained a relative improvement in the overall Continuous Ranked Probability Score (CRPS) of 17.1% on Australian domestic tourism data, 24.2% on the Favorita grocery sales dataset, and 6.9% on a San Francisco Bay Area highway traffic dataset.

*Keywords:* Probabilistic Hierarchical Forecasting, Neural Networks, Poisson Mixtures

---

## 1. Introduction and Motivation

We study the task of hierarchical time series forecasting where forecast users need probabilistic predictions for all related time series organized into a hierarchy or group structure (Hyndman et al., 2014; Athanasopoulos et al., 2017; Spiliotis et al., 2020). As predictions for different aggregation levels drive different decisions, forecast coherence is desirable to ensure aligned decision-making across the hierarchies (Fotios Petropoulos et. al., 2021). Notable examples of hierarchical forecasting tasks include the necessity from energy planners to synchronize the electricity load at each level of the grid with total production (Ben Taieb &

---

\*Corresponding author

*Email address:* meeteio@amazon.com (O. Nganba Meetei)

Koo, 2019; Jeon et al., 2019), the short-term load forecasting category in the Global Energy Forecasting Competition 2012 (GEFCOM2012; Hong et al. 2014), and the research efforts from forecasting community and retailers manifested at the fifth Makridakis Competition (M5; Makridakis et al. 2020).

Coherent forecasts are defined as those that satisfy the aggregation constraints of the hierarchy. That is, dis-aggregated predictions “add up” to the predictions of aggregate levels. This definition is easy to understand for mean forecasts, which are additive. For probabilistic forecasts, it means that the predictive distribution of the aggregate series is equal to the distribution of the sum of its children series (Taieb et al., 2017; Puwasala et al., 2018). Probabilistic coherence is guaranteed when marginal distributions come from a joint distribution shared across all the aggregation levels (Taieb et al., 2017; Jeon et al., 2019).

The main challenge in probabilistic hierarchical time series forecasting is to utilize relationships between time series across all levels to produce accurate and coherent forecasts. There is a large body of work on Bayesian hierarchical<sup>1</sup> modeling of Spatio-temporal data; its predictions by construction are coherent (Wikle et al., 1998; Diggle, 2013). These models, however, come with strong assumptions, as they typically assume a stationary Gaussian process to induce correlations and rely on Markov Chain Monte Carlo to estimate the posterior distribution (Diggle & Brix, 2001; Diggle, 2013). For modeling count data, variants of Bayesian Hierarchical Poisson Regression Models were introduced (Christiansen & Morris, 1997; Park & Lord, 2009), but they usually come with linearity assumptions. Scaling these models up to high dimensional problems can be computationally expensive as well. Black-box methods like neural networks, on the other hand, are computationally efficient and can generate accurate forecasts (Wen et al., 2017). However, hierarchical coherence is generally not guaranteed in neural network models.

Hierarchical forecast reconciliation strategies provide an interesting approach for bringing back hierarchical coherence into neural forecasting methods. Early work focused on reconciling independently generated base forecasts for the mean at different levels (Hyndman et al., 2011; Wickramasuriya et al., 2019). The reconciliation strategies improved accuracy, and recently a better understanding of the reconciliation process was provided through the language of forecast combinations (Hollyman et al., 2021). Similar two-step forecast reconciliation methods were later extended to probabilistic forecasts as well (Taieb et al., 2017; Puwasala et al., 2018), first estimating the marginal distributions independently and then reconciling them. More recent work by Han et al. (2021) and Rangapuram et al. (2021) proposed combining these two steps into a single neural network. Separately, Puwasala et al. (2018) suggest that the accuracy improvements seen in point forecast reconciliation will also extend to probabilistic forecast reconciliations.

In this work, we present a novel method for producing coherent probabilistic forecasts. It combines the strength of modern neural networks and an intuitive statistical model for the joint distribution. In contrast to earlier efforts (Han et al., 2021; Rangapuram et al., 2021),

---

<sup>1</sup>Note that the term hierarchy in Bayesian hierarchy is different from its use in hierarchical forecasting. The former refers to the conditional dependence of model parameters’ posterior distribution, and the latter refers to the aggregation constraints across multiple time series.

our approach is a *Mixture Density Network* (MDN; Bishop 1994). Our method is coherent by construction and does not require an explicit re-conciliation step, either as part of a single end-to-end network or as a separate step. We call it the *Deep Poisson Mixture Network* (DPMN). The DPMN models the joint probability of the multivariate time series as a finite mixture of Poisson distributions and combines that with the well-established **MQ-Forecaster** neural architecture (Wen et al., 2017; Eisenach et al., 2021). This is possible because we formulate the problem as an MDN, and we can choose a relevant class of probabilistic distributions for the statistical model and the neural architecture independently. The key advantages of our method are:

1. **Flexible Predictive Distribution:** We model the predictive distribution as a finite mixture of Poisson random variables, which is analogous to a kernel density with Poisson kernels. The resulting distribution is flexible, capable of accurately modeling a wide range of probability distributions, and compatible as an output layer with state-of-the-art neural architectures. We will demonstrate this empirically on three different forecasting tasks in Section 6.
2. **Computational Efficiency:** Learning coherent forecast distributions in a high dimensional hierarchical space can be computationally intractable. To alleviate this, we anchor the DPMN on a joint distribution of the bottom level time series and employ optimization strategies based on composite likelihoods, which enables us to extend to large-scale applications.

The rest of the work is structured as follows. In Section 2 we introduce mathematical notation and review in greater detail the literature on the *statistical* and *neural-network* based solutions. We describe the probabilistic model used in our method in Section 3 and the learning and inference methods in Section 4. In Section 5 we discuss the neural network architecture and in Section 6 we perform an empirical evaluation, where we showcase the unique characteristics and advantages of our method when compared to other probabilistically coherent models. Finally, in Section 7 we discuss future work and conclude.

## 2. Literature Review

### 2.1. Hierarchical Forecasting Notation

Mathematically a hierarchical multivariate time series can be denoted by the vector  $\mathbf{y}_{[a,b],\tau} = [\mathbf{y}_{[a],\tau}^\top \mid \mathbf{y}_{[b],\tau}^\top]^\top \in \mathbb{R}^{(N_a+N_b)}$  for each time point  $\tau$ ; where  $[a], [b]$  stand for all aggregate and bottom indices of the time series respectively. The total number of series in the hierarchy is  $|[a, b]| = (N_a + N_b)$ , where  $|[a]| = N_a$  is the number of aggregated series and  $|[b]| = N_b$  the number of bottom series that are at the most dis-aggregated level possible. Time indices for past information until  $t$  is given by the set  $[t]$  with length  $|[t]| = N_t$ , and the  $h$  time step forecast horizon is denoted as  $[t + 1 : t + h]$ . With this notation the hierarchical aggregation constraints at each time point  $\tau \in [t]$  have the following matrix representation:

$$\mathbf{y}_{[a,b],\tau} = \mathbf{H}\mathbf{y}_{[b],\tau} \quad \Leftrightarrow \quad \begin{bmatrix} \mathbf{y}_{[a],\tau} \\ \mathbf{y}_{[b],\tau} \end{bmatrix} = \begin{bmatrix} \mathbf{S}_{[a][b]} \\ \mathbf{I}_{[b][b]} \end{bmatrix} \mathbf{y}_{[b],\tau} \quad (1)$$

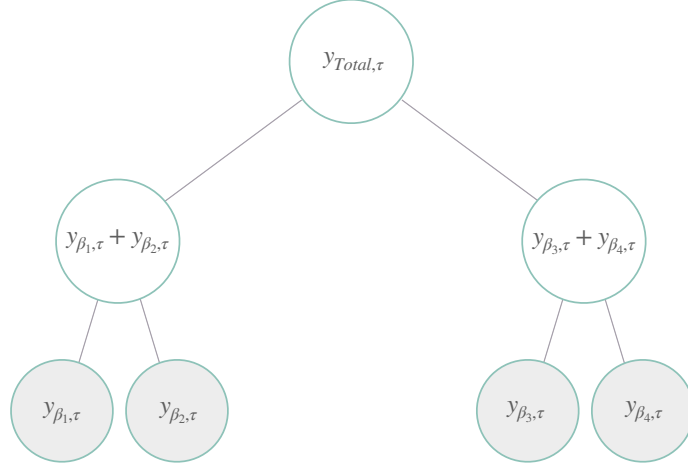


Figure 1: A simple three level time series hierarchical structure, with four bottom level variables. The disaggregated bottom variables are marked with gray background. In this description each node represents non overlapping series for a single point in time.

The matrix  $\mathbf{H} \in \mathbb{R}^{(N_a+N_b) \times N_b}$  aggregates the bottom level series to the series above. It is composed by vertically stacking a summing matrix  $\mathbf{S}_{[a][b]} \in \mathbb{R}^{N_a \times N_b}$  and an identity matrix  $\mathbf{I}_{[b][b]} \in \mathbb{R}^{N_b \times N_b}$ .

For example, Figure 1 represents a simple hierarchy where each parent node is the sum of its children. Here the dimensions are  $N_a = 3$ ,  $N_b = 4$ , and the hierarchical, aggregated and base series are respectively:

$$\begin{aligned}
 y_{\text{Total}, \tau} &= y_{\beta_1, \tau} + y_{\beta_2, \tau} + y_{\beta_3, \tau} + y_{\beta_4, \tau} \\
 \mathbf{y}_{[a], \tau} &= [y_{\text{Total}, \tau}, y_{\beta_1, \tau} + y_{\beta_2, \tau}, y_{\beta_3, \tau} + y_{\beta_4, \tau}]^\top & \mathbf{y}_{[b], \tau} &= [y_{\beta_1, \tau}, y_{\beta_2, \tau}, y_{\beta_3, \tau}, y_{\beta_4, \tau}]^\top
 \end{aligned} \tag{2}$$

The constraint matrix of the Figure 1 example and the corresponding aggregations from Equation (2) are as following:

$$\mathbf{H} = \begin{bmatrix} \mathbf{S}_{[a][b]} \\ \mathbf{I}_{[b][b]} \end{bmatrix} = \begin{bmatrix} 1 & 1 & 1 & 1 \\ 1 & 1 & 0 & 0 \\ 0 & 0 & 1 & 1 \\ \hline 1 & 0 & 0 & 0 \\ 0 & 1 & 0 & 0 \\ 0 & 0 & 1 & 0 \\ 0 & 0 & 0 & 1 \end{bmatrix}$$

## 2.2. Reconciliation Strategies

Most of the prior statistical solutions to the hierarchical forecasting challenge implement a two-stage process, where first a set of base forecasts  $\hat{\mathbf{y}}_{[a,b],\tau} \in \mathbb{R}^{N_a+N_b}$  are created and then revised into coherent forecasts  $\tilde{\mathbf{y}}_{[a,b],\tau}$  through a reconciliation method. The reconciliation can be compactly expressed by

$$\tilde{\mathbf{y}}_{[a,b],\tau} = \mathbf{H}\mathbf{P}\hat{\mathbf{y}}_{[a,b],\tau} \quad (3)$$

where  $\mathbf{H} \in \mathbb{R}^{(N_a+N_b) \times N_b}$  is the hierarchical aggregation matrix and  $\mathbf{P} \in \mathbb{R}^{N_b \times (N_a+N_b)}$  is a projection matrix determined by the reconciliation strategies. The most common reconciliation methods can be classified into *top-down*, *bottom-up* and *alternative* approaches.

- Bottom-up: The simple *bottom-up* strategy, abbreviated as **NaiveBU** (Orcutt et al., 1968), first generates bottom level forecasts and then aggregates them to produce predictions for all the series in the hierarchical structure.
- Top-down: The *top-down* strategy, abbreviated as **TD** (Gross & Sohl, 1990; Fliedner, 1999), distributes the total forecast, and then disaggregates it down the hierarchy using proportions that can be historical actuals or forecasted separately.
- Alternative: The more recent *middle-out* strategies, denoted as **MO** (Hyndman et al., 2011; Hyndman & Athanasopoulos, 2018)), treat the second stage reconciliation as an optimization problem for the projection matrix  $\mathbf{P}$ . These reconciliation techniques include among others *Game-Theoretically OPTimal* (**GTOP**; Van Erven & Cugliari 2015), learning a projection for reducing quadratic loss, a generalized least squares model for minimizing trace of the squared error matrix, namely the *minimum trace* reconciliation (**MinT**; Wickramasuriya et al. 2019) and the *empirical risk minimization* approach (**ERM**; Ben Taieb & Koo 2019).

Despite the advancements in alternative reconciliation strategies with statistical solutions, as mentioned in Section 1, there are still fundamental limitations. First, most post-process reconciliation methods produce mean forecasts but not probabilistic forecasts, with some exceptions that rely on strong Gaussian noise assumptions that can be restrictive (Gneiting & Katzfuss, 2014; Taieb et al., 2017; Panagiotelis et al., 2020). Second, the mentioned methods learn the model parameters of the base level forecasts independently, and the induced data scarcity translates into a missed opportunity to share a common expressive model that leverages the power of nonlinear transformations of the data.

### 2.3. Hierarchical Neural Forecasting

In the last decade, neural network-based forecasting methods have become ubiquitous in large-scale forecasting applications (Wen et al., 2017; Böse et al., 2017; Madeka et al., 2018; Eisenach et al., 2021), transcending industry boundaries into academia, as it has redefined the state-of-the-art in many practical tasks (Yu et al., 2018; Ravuri et al., 2021; Olivares et al., 2021) and forecasting competitions (Makridakis et al., 2018, 2020).

The latest neural network-based solutions to the hierarchical forecasting challenge include methods like the *Simultaneous Hierarchically Reconciled Quantile Regression* (SHARQ; Han et al. 2021) and *Hierarchically Regularized Deep Forecasting* (HIRED; Paria et al. 2021) that augment the training loss function with approximations to the hierarchical constraints. And *Hierarchical End-to-End* learning (HierE2E; Rangapuram et al. 2021) that integrates an alternative reconciliation strategy in its predictions through linear projections. With the exception of HierE2E, the rest of these methods encourage probabilistic hierarchical coherence through regularization but do not guarantee it. Additionally, if a user requires updating the hierarchical structure of interest, a whole new optimization of the networks would be needed for the existing methods to forecast the structure correctly.

As mentioned in Section 1, the computational efficiency of the available hierarchical neural architectures can be a considerable hurdle as none of the methods are readily usable for large-scale applications. The methods cannot capitalize on all available scaling innovations for deep learning architectures; one such example is the *forking-sequences* technique that enables the **MQ-Forecaster** model family to scale well to large datasets (Wen et al., 2017).

Our proposed method, DPMN, addresses these deficiencies by specifying the output contract to be a finite Poisson mixture, and is flexible to the deep learning architectures underlying it. Using this output contract, a model needs only to forecast the bottom-most level in the hierarchy, after which any desired hierarchical structure of interest can be forecasted with guaranteed probabilistic hierarchical coherence. The DPMN model with Poisson distributional assumption on observed data was primarily motivated by count data, but the model family can be extended to answer other time series forecasting problems.

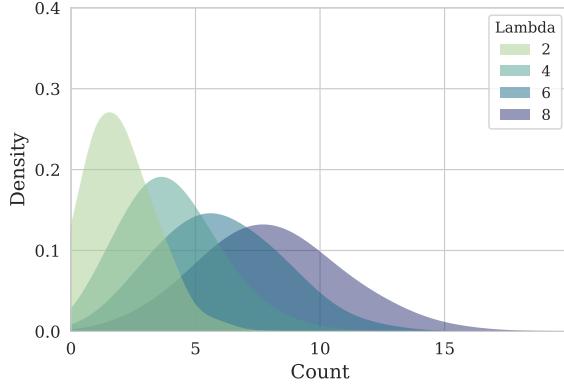


Figure 2: The Poisson Mixture distribution has desirable properties that make it well-suited for probabilistic hierarchical forecasting for count data. Under minimal conditions, its aggregation rule implies probabilistic coherence of the random variables it models.

### 3. Probabilistic Model

#### 3.1. Joint Poisson Mixture Distribution

We start by postulating that the joint distribution of future multivariate time series  $\mathbf{y}_{[b][t+1:t+h]} \in \mathbb{N}^{N_b \times h}$  is captured by a Poisson mixture:

$$P(\mathbf{y}_{[b][t+1:t+h]}) = \int_{\boldsymbol{\lambda}} (P(\boldsymbol{\lambda}_{[b][t+1:t+h]}) \prod_{(\beta, \tau) \in [b][t+1:t+h]} \text{Poisson}(y_{\beta, \tau} | \lambda_{\beta, \tau})) d\boldsymbol{\lambda}_{[b][t+1:t+h]} \quad (4)$$

Equation (4) assumes that observations are conditionally independent given the Poisson rates

$$y_{\beta, \tau} | \lambda_{\beta, \tau} \perp\!\!\!\perp y_{\beta', \tau'} | \lambda_{\beta', \tau'} \quad (5)$$

for all  $(\beta, \tau) \neq (\beta', \tau')$  and  $(\beta, \tau), (\beta', \tau') \in [b][t+1:t+h]$ , and all dependencies in the observations are captured by the joint distribution of the Poisson rates  $\boldsymbol{\lambda}_{[b][t+1:t+h]}$ . The setup so far is similar to a standard Bayesian hierarchical formulation. However, instead of assuming a parametric model like Gaussian process that drives the latent variables, with the DPMM we approximate the joint distribution of the Poisson rates by a finite mixture of weighted multi-variate samples

$$P(\boldsymbol{\lambda}_{[b][t+1:t+h]}) = \sum_{\kappa=1}^{N_k} w_{\kappa} \prod_{(\beta, \tau) \in [b][t+1:t+h]} \delta(\lambda_{\beta, \tau} - \lambda_{\beta, \kappa, \tau}) \quad (6)$$

where  $\delta(x)$  is the Dirac Delta function. The Poisson rates  $\boldsymbol{\lambda}_{[b][k][t+1:t+h]} \in \mathbb{R}^{N_b \times N_k \times h}$  and the associated weights  $\mathbf{w}_{[k]} \in \mathbb{R}^{N_k}$ , with  $\mathbf{w}_{[k]} \geq 0$  and  $\sum_{\kappa=1}^{N_k} w_{\kappa} = 1$ , are parameters of the probability distribution to be estimated. The number of Poisson components  $|[k]| = N_k$  is a hyperparameter of the model that controls the fidelity of the mixture distribution.

The predictive distribution for  $\mathbf{y}_{[b][t+1:t+h]}$  in DPMN is

$$P(\mathbf{y}_{[b][t+1:t+h]}) = \sum_{\kappa=1}^{N_k} w_{\kappa} \prod_{(\beta,\tau) \in [b][t+1:t+h]} \left( \frac{(\lambda_{\beta,\kappa,\tau})^{y_{\beta,\tau}} \exp\{-\lambda_{\beta,\kappa,\tau}\}}{(y_{\beta,\tau})!} \right) \quad (7)$$

The resulting model can be interpreted as a multivariate kernel density approximation, with Poisson kernels, to the actual probability distribution. It can also be thought of as a latent variable model. We show an example of the Poisson mixture distribution in Figure 2.

### 3.2. Marginal Distributions for Bottom Series

Equation (7) describes the joint distribution of all bottom level time series. We can derive forecasts for one of the bottom level series  $\beta \in [b]$  for a single future time period  $\tau \in [t+1 : t+h]$  via a marginal distribution. After integrating out the remaining time and series indices, the marginal distribution is:

$$P(y_{\beta,\tau}) = \sum_{\kappa=1}^{N_k} w_{\kappa} \left( \frac{(\lambda_{\beta,\kappa,\tau})^{y_{\beta,\tau}} \exp\{-\lambda_{\beta,\kappa,\tau}\}}{(y_{\beta,\tau})!} \right) \quad (8)$$

The final expression is equivalent to simply dropping all other time series and time periods from the product in Equation (7).

### 3.3. Marginal Distributions for Aggregate Series

An important consequence of the *conditional independence* is that computing the predictive distributions at aggregate levels  $\mathbf{y}_{[a],\tau}$  depends on a simple component-wise addition of the lower level Poisson rates. This can be described as  $\boldsymbol{\lambda}_{[a][k],\tau} = \mathbf{S}_{[a][b]} \boldsymbol{\lambda}_{[b][k],\tau}$  with  $\mathbf{S}_{[a][b]}$  the hierarchical summation matrix defined in Section 2.1. Then for any aggregate level  $\alpha \in [a]$  and time  $\tau \in [t+1 : t+h]$ , the marginal distribution is:

$$P(y_{\alpha,\tau}) = \sum_{\kappa=1}^{N_k} w_{\kappa} \left( \frac{(\lambda_{\alpha,\kappa,\tau})^{y_{\alpha,\tau}} \exp\{-\lambda_{\alpha,\kappa,\tau}\}}{(y_{\alpha,\tau})!} \right) \quad (9)$$

The predictive distributions are hierarchically coherent by construction.

### 3.4. Covariance Matrix

Using the law of total covariance and the conditional independence in Equation (5), the covariance of any two bottom level series naturally follows:

$$\text{Cov}(y_{\beta,\tau}, y_{\beta',\tau'}) = \sum_{\kappa=1}^{N_k} w_{\kappa} (\lambda_{\beta,\kappa,\tau} - \bar{\lambda}_{\beta,\tau}) (\lambda_{\beta',\kappa,\tau'} - \bar{\lambda}_{\beta',\tau'}) \quad (10)$$

for all  $(\beta, \tau), (\beta', \tau') \in [b][t+1 : t+h]$  and  $\bar{\lambda}_{\beta,\tau} = \sum_{\kappa \in [k]} w_{\kappa} \lambda_{\beta,\kappa,\tau}$ .



## 4. Parameter Estimation and Inference

### 4.1. Maximum Joint Likelihood

To estimate model parameters, we can maximize the joint likelihood implied by the joint distribution from Equation (7). Let  $\boldsymbol{\theta}$  represent the neural network parameters as described in Section 5, we parameterize the probabilistic model as follows:

$$\begin{aligned}\boldsymbol{\lambda}_{[b][k][t+1:t+h]} &:= \hat{\boldsymbol{\lambda}}_{[b][k][t+1:t+h]}(\boldsymbol{\theta} \mid \mathbf{y}_{[b][:t]}, \mathbf{x}_{[b][:t]}^{(h)}, \mathbf{x}_{[b][t+1:t+h]}^{(f)}, \mathbf{x}_{[b]}^{(s)}) \\ \mathbf{w}_{[k]} &:= \hat{\mathbf{w}}_{[k]}(\boldsymbol{\theta} \mid \tilde{\mathbf{x}}_{[:t]}^{(h)}, \tilde{\mathbf{x}}^{(s)})\end{aligned}\quad (11)$$

where the Poisson rates  $\boldsymbol{\lambda}_{[b][k][t+1:t+h]}$  are conditioned on  $\mathbf{y}_{[b][:t]}$ ,  $\mathbf{x}_{[b][:t]}^{(h)}$ ,  $\mathbf{x}_{[b][t+1:t+h]}^{(f)}$ ,  $\mathbf{x}_{[b]}^{(s)}$  the history of the bottom level time series, other associated historical covariates, future information available at the time of prediction and static features. And the shared mixture weights  $\mathbf{w}_{[k]}$ , are conditioned on temporal and static aggregate features shared across the bottom series,  $\tilde{\mathbf{x}}_{[:t]}^{(h)} \subset \mathbf{x}_{[:t]}^{(h)}$  and  $\tilde{\mathbf{x}}^{(s)} \subset \mathbf{x}_{[b]}^{(s)}$ .

We denote the combined conditioning information as

$$\mathbf{x}_{[:\tau]}^{(h)} = \{\mathbf{x}_{[b][:\tau]}^{(h)}, \tilde{\mathbf{x}}_{[:\tau]}^{(h)}\} \quad \text{and} \quad \mathbf{x}^{(s)} = \{\mathbf{x}_{[b]}^{(s)}, \tilde{\mathbf{x}}^{(s)}\} \quad (12)$$

The negative log-likelihood can then be written<sup>2</sup>:

$$\mathcal{L}(\boldsymbol{\theta}) = -\log \left[ \sum_{\kappa=1}^{N_k} \hat{w}_{\kappa}(\boldsymbol{\theta}) \prod_{(\beta, \tau) \in [b][t+1:t+h]} \left( \frac{(\hat{\lambda}_{\beta, \kappa, \tau}(\boldsymbol{\theta}))^{y_{\beta, \tau}} \exp\{-\hat{\lambda}_{\beta, \kappa, \tau}(\boldsymbol{\theta})\}}{(y_{\beta, \tau})!} \right) \right] \quad (13)$$

The maximum likelihood estimation method (MLE) has desirable properties like statistical efficiency and consistency. However, the mixture components cannot be estimated separately, for this reason, MLE is only feasible for hierarchical time series with a small number of series and additional exploration is needed to make the estimation scalable.

### 4.2. Maximum Composite Likelihood

An attractive, computationally efficient alternative to MLE for estimating the model parameters is to maximize the composite likelihood. This method involves breaking up the high-dimensional space into smaller sub-spaces, and the composite likelihood consists of the weighted product of the marginal likelihoods of the subspaces (Lindsay, 1988). For simplicity, we used uniform weights.

In addition to the computational efficiency, maximizing the composite likelihood provides a robust and unbiased estimate of marginal model parameters with the drawback that the model inference may suffer from properties of a misspecified model (Varin et al., 2011). We will discuss variants of the composite likelihood below.

---

<sup>2</sup>We kept notations simple and omitted the explicit conditioning on input features.

#### 4.2.1. Naive Bottom Up

A simple option of using composite likelihood is to define each bottom-level time series as its likelihood sub-space and treat them as independent during model training (Orcutt et al., 1968). We refer to this estimation method for the DPMN as *Naive Bottom Up* (DPMN-NaiveBU). The negative logarithm of the DPMN-NaiveBU composite likelihood follows:

$$\mathcal{L}_{\text{NaiveBU}}(\boldsymbol{\theta}) = - \sum_{\beta \in [b]} \log \left[ \sum_{\kappa=1}^{N_k} \hat{w}_{\kappa}(\boldsymbol{\theta}) \prod_{\tau \in [t+1:t+h]} \left( \frac{(\hat{\lambda}_{\beta,\kappa,\tau}(\boldsymbol{\theta}))^{y_{\beta,\tau}} \exp \{-\hat{\lambda}_{\beta,\kappa,\tau}(\boldsymbol{\theta})\}}{(y_{\beta,\tau})!} \right) \right] \quad (14)$$

This model still learns time correlations within a single series and will generate coherent forecast distributions for aggregations in the time dimension. It does not attempt, however, to discover correlations across different time series.

#### 4.2.2. Group Bottom Up

If prior information helps us identify groups of time series with interesting correlation structures, we may estimate them by including the groups in the composite likelihood. We refer to this estimation method for the DPMN as *Group Bottom Up* (DPMN-GroupBU). Let  $\mathcal{G} = \{[g_i]\}$  be time-series groups, then the negative log composite likelihood for the DPMN-GroupBU is

$$\mathcal{L}_{\text{GroupBU}}(\boldsymbol{\theta}) = - \sum_{[g_i] \in \mathcal{G}} \log \left[ \sum_{\kappa=1}^{N_k} \hat{w}_{\kappa}(\boldsymbol{\theta}) \prod_{(\beta,\tau) \in [g_i][t+1:t+h]} \left( \frac{(\hat{\lambda}_{\beta,\kappa,\tau}(\boldsymbol{\theta}))^{y_{\beta,\tau}} \exp \{-\hat{\lambda}_{\beta,\kappa,\tau}(\boldsymbol{\theta})\}}{(y_{\beta,\tau})!} \right) \right] \quad (15)$$

The main advantage over DPMN-NaiveBU is that the model now learns to capture the cross-temporal relationships. One must take care when defining the time-series groups to maximize the benefits for the DPMN-GroupBU estimation method.

#### 4.3. Forecast Inference

As mentioned earlier, model inference from composite likelihood estimation suffers from model misspecification problems. If we use the DPMN-NaiveBU model for prediction, the model does not understand the covariance structure defined in Equation (10). To recover the joint distribution in Equation (7) we need a method for relating the marginal distributions learnt from the maximum composite likelihood method to one another. Here our choice of sharing sample weights  $\mathbf{w}_{[k]}$  across all marginal distributions provide a natural scheme. We identify Poisson components with the same weight as part of a multivariate sample in the high dimensional space. In other words, we define a *component matching method* where we associate the first mixture component for  $\beta \in [b]$  with the first mixture component for any other  $\beta' \in [b]$ , the second component of  $\beta$  with the second component of  $\beta'$  and so on. With such mapping defined, recovering the joint distribution is trivial. This method of associating mixture components may look like a forecast reconciliation step, but it is different from the notion of forecast reconciliation used in other hierarchical forecasting

methods to fix incoherence. We are not trying to fix incoherence, instead, we are filling in missing information in the model without any additional computational cost.

For the **DPMN-NaiveBU** estimation method, the component matching method is definitely a stretch. We are filling in a lot of missing information. The **DPMN-GroupBU** approach significantly alleviates this problem because the model parameters are well defined within each group  $[g_i] \in \mathcal{G}$  and if most of the interesting correlations are already captured within each group, then much less burden is placed on the component matching method. We show in the empirical evaluation of Section 6 that both **DPMN-NaiveBU** and **DPMN-GroupBU** models perform favorably when compared to other hierarchical forecasting methods, and between the two, **DPMN-GroupBU** is better when the grouping given is informative while **DPMN-NaiveBU** is better when the grouping given is less informative.

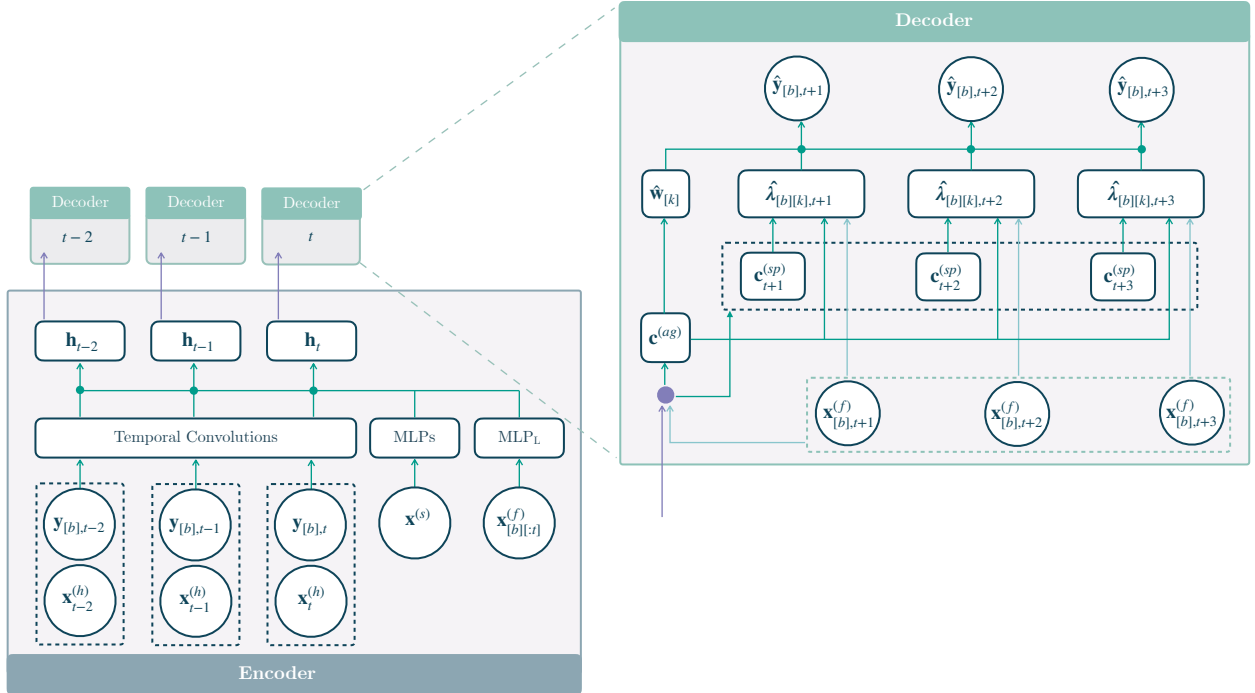


Figure 3: The *Deep Poisson Mixture Network* (DPMN) is a *Sequence-to-Sequence with Context* network that uses dilated temporal convolutions as the primary encoder and multilayer perceptron based decoders for a direct multi-horizon forecast. The forked decoders share their parameters and create the multi-horizon predictions for each time point in the encoder, making the architecture efficient in its optimization and predictions.

## 5. Deep Poisson Mixture Network

Our primary goal is to create a probabilistic hierarchical forecasting model that is accurate and efficient. For this purpose, we opted to extend the proven **MQ-Forecaster** family (Wen et al., 2017; Eisenach et al., 2021) with the discrete Poisson mixture distribution. We refer to this model as *Deep Poisson Mixture Network* (DPMN).

### 5.1. Model Architecture

In summary, the DPMN builds on the **MQ-Forecaster** architecture that is based on *Sequence-to-Sequence with Context* network (**Seq2SeqC**; Cho et al. (2014)). The DPMN uses dilated temporal convolutions (**TempConv**; van den Oord et al. (2016)) to encode the available history into hidden states and uses forked decoders based on *Multi-Layer Perceptron* (**MLP**; Rosenblatt (1961)) in a direct multi-horizon forecast strategy (Atiya & Taieb, 2016). We describe below in further detail the components of the model. Details on the model hyperparameters such as layer dimensions, are available in Table A4.

### 5.1.1. Encoder

As explained earlier the DPMN main encoder is a stack of dilated temporal convolutions. Additionally, we use a global dense layer to encode the static features and a local dense layer, shared across time, to encode the available future information. The encoder for each time  $\tau \in [t]$  and its components are described in Equation (16).

$$\begin{aligned} \mathbf{h}_\tau^{(h)} &= \{\mathbf{h}_{1,\tau}^{(h)}, \tilde{\mathbf{h}}_{2,\tau}^{(h)}\} = \{\mathbf{TempConv}(\mathbf{x}_{[b]:[\tau]}^{(h)}), \mathbf{TempConv}(\tilde{\mathbf{x}}_{[\tau]}^{(h)})\} \\ \mathbf{h}_\tau^{(s)} &= \{\mathbf{h}_1^{(s)}, \mathbf{h}_2^{(s)}\} = \{\mathbf{MLP}(\mathbf{x}_{[b]}^{(s)}), \mathbf{MLP}(\tilde{\mathbf{x}}^{(s)})\} \\ \mathbf{h}_\tau^{(f)} &= \mathbf{MLP}_L(\mathbf{x}_{[b]:[\tau+h]}^{(f)}) \end{aligned} \quad (16)$$

where we distinguish the input features  $\mathbf{x}_{[\tau]}^{(h)} = \{\mathbf{x}_{[b]:[\tau]}^{(h)}, \tilde{\mathbf{x}}_{[\tau]}^{(h)}\}$  into bottom level and shared historical covariates respectively. As well for  $\mathbf{x}^{(s)} = \{\mathbf{x}_{[b]}^{(s)}, \tilde{\mathbf{x}}^{(s)}\}$  the bottom level and shared static features.

The encoder's output in Equation (17) is a set of shared and bottom level encoded features  $\mathbf{h}_{1,\tau}$  and  $\mathbf{h}_{2,\tau}$ . The first concatenates all the encoded past  $\mathbf{h}_{1,\tau}^{(h)}, \mathbf{h}_{2,\tau}^{(h)} \in \mathbb{R}^{N_{cf}}$ , static  $\mathbf{h}_1^{(s)}, \mathbf{h}_2^{(s)} \in \mathbb{R}^{N_s}$  and available future  $\mathbf{h}_\tau^{(f)} \in \mathbb{R}^{N_f}$  information. The second one concatenates the encoded past  $\mathbf{h}_{2,\tau}^{(p)} \in \mathbb{R}^{N_p}$ , and static  $\mathbf{h}_2^{(s)} \in \mathbb{R}^{N_s}$  shared features.

$$\mathbf{h}_\tau = \{\mathbf{h}_{1,\tau}, \mathbf{h}_{2,\tau}\} = \{[\mathbf{h}_{1,\tau}^{(h)}|\mathbf{h}_{2,\tau}^{(h)}|\mathbf{h}_1^{(s)}|\mathbf{h}_2^{(s)}|\mathbf{h}_\tau^{(f)}], [\mathbf{h}_{2,\tau}^{(h)}|\mathbf{h}_2^{(s)}]\} \quad (17)$$

### 5.1.2. Forked Decoders

The DPMN uses a two-branch MLP decoder. The first decoder branch, summarizes the encoder output and future available information into two contexts: The horizon-agnostic context set  $\mathbf{c}^{(ag)} \in \mathbb{R}_{ag}^N$  and the horizon-specific context  $\mathbf{c}_{[\tau+1:\tau+h]}^{(sp)} \in \mathbb{R}^{N_{sp} \times h}$  that provides structural awareness of the forecast horizon and plays a crucial role in expressing recurring patterns in the time series if any. Equation (18) describes the first decoder branch:

$$\begin{aligned} \mathbf{c}^{(ag)} &= \{\mathbf{c}_1^{(ag)}, \mathbf{c}_2^{(ag)}\} = \{\mathbf{MLP}(h_{1,\tau}), \mathbf{MLP}(h_{2,\tau})\} \\ \mathbf{c}_{[\tau+1:\tau+h]}^{(sp)} &= \mathbf{MLP}_L(h_{1,\tau}) \end{aligned} \quad (18)$$

The second decoder branch adapts the horizon-specific and horizon-agnostic contexts into the parameters of the Poisson mixture distribution. For the horizon-specific Poisson rates, we use the forking-sequence technique with a series of decoders with shared parameters for each time point  $\tau \in [t]$  and for the mixture weights, we apply an MLP followed by a softmax on the aggregate horizon agnostic context. Equation (19) describes the second decoder branch:

$$\begin{aligned} \hat{\boldsymbol{\lambda}}_{[b][k][t+1:t+h]} &= \mathbf{MLP}_L(\mathbf{c}_1^{(ag)}, \mathbf{c}_{[\tau+1:\tau+h]}^{(sp)}, \mathbf{x}_{[b]:[\tau+h]}^{(f)}) \\ \hat{\mathbf{w}}_{[k]} &= \text{SoftMax}(\mathbf{MLP}(\mathbf{c}_2^{(ag)})) \end{aligned} \quad (19)$$

Table 1: Summary, hierarchical structure and forecast horizon of datasets used in our empirical study.

DATASET	TOTAL	AGGREGATED	BOTTOM	LEVELS	OBSERVATIONS	HORIZON ( $h$ )
TRAFFIC	207	7	200	4	366	1
TOURISM-L	555	175	76/304	4/5	228	12
FAVORITA	371,312	153,386	217,944	4	1,688	34

## 6. Empirical Evaluation

To evaluate our method, we consider three forecasting tasks where the objective is to predict quantile forecasts for each time series in the group or hierarchical structure. All the three datasets that we use in the empirical evaluation<sup>3</sup> are publicly available and have been used in hierarchical forecasting literatures (Wickramasuriya et al., 2019; Ben Taieb & Koo, 2019; Rangapuram et al., 2021; Paria et al., 2021).

**Traffic** (Dua & Graff, 2017) measures the occupancy of 963 car lanes in the San Francisco Bay Area freeways from January 2008 to March 2009. The data was grouped by Ben Taieb & Koo (2019) into a year of daily observations, consisting of a 207 series hierarchical structure. **Tourism-L** (Tourism Australia, Canberra, 2019) is an Australian Tourism dataset from a national visitor survey, managed by Tourism Research Australia. The dataset contains 555 monthly series from 1998 to 2016, grouped by geography and purposes of travel. **Favorita** (Corporación Favorita, 2018) is a Kaggle competition dataset of grocery item sales daily history with additional information on promotions, items, stores and holidays. The balanced dataset contains 371,312 series from January 2013 to August 2017. We define a geographic hierarchy with states, cities, and stores. Table 1 summarizes the characteristics of the datasets; we defer a detailed description to Appendix A.1.

The datasets provide an opportunity to showcase the broad applicability of the DPMN, as each has unique characteristics. **Tourism-L** allows us to test the DPMN to model group structures with multiple hierarchies. **Favorita** allows us to test the DPMN on a large-scale dataset. **Traffic** is composed of randomly assigned hierarchical groupings that may not have any informative structures for the DPMN to learn with **GroupBU**. Finally, **Favorita** contains some non-count demand values (for instance, weights of produce) and **Traffic** aggregated occupancy rates are non-count data, so modeling these datasets with a Poisson mixture limits the maximum accuracy we can achieve.

### 6.1. Datasets Partition and Preprocessing

We consider the following *partition* for the three datasets: we hold out the final horizon-length observations as the *test set*. In a rolling-window fashion, we use the horizon-length observations that precede the *test set* as the *validation test* and treat as *training set* the rest of the past information. A *partition* example is depicted in Figure 4.

<sup>3</sup>**Traffic** is available at the [UCI ML repository](#). **Tourism-L** is available at [MinT reconciliation web page](#). **Favorita** is available in its [Kaggle Competition url](#).

For comparability purposes with the most recent hierarchical forecasting literature, we keep ourselves as close as possible to the preprocessing and wrangling of the datasets to that of Rangapuram et al. (2021)<sup>4</sup>. In general, the *static* variables that we consider on all the datasets correspond to the hierarchical and group designators as categorical variables implied by the hierarchical constraint matrix. The *temporal* covariates that we consider are the time series for the upper levels of the hierarchy, as well as calendar covariates associated with the time series frequency of each dataset. As *future* information, we include calendar covariates to help the DPMN capture seasonal patterns.

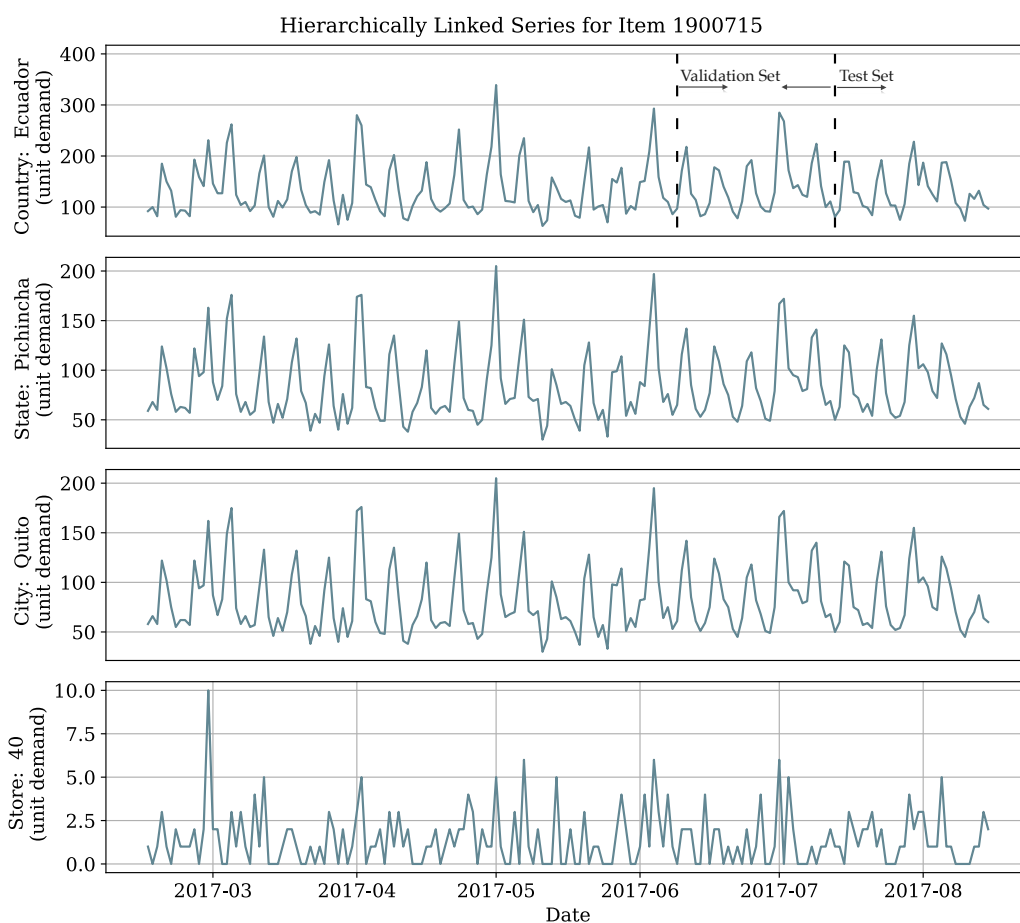


Figure 4: Example of a geographically linked time series from the **Favorita** dataset. The top level shows the sales for a grocery item for the Favorita stores in the country of Ecuador. The second level shows the sold units within the Pichincha state, the third level shows the sales for the city of Quito, the final level shows the sales for the item at a particular store. For this dataset, the training set comprises all the observations preceding the validation and test sets. The validation set (between the first and second dotted lines) is the 34 days before the test set. The held-out test set (marked by the last dotted line) is the last 34 observations.

<sup>4</sup>The pre-processed datasets are available in the hierarchical forecasting extension to the [GluonTS library](#).

Table 2: Considered hyperparameters for the *Deep Poisson Mixture Network* (DPMN). The learning rate, random seed, and SGD epochs that performed best on the validation set were selected automatically in each HYPEROPT run. Model architecture parameters and batch size were configured once per dataset, as explained in Table A4.

HYPERPARAMETER	CONSIDERED VALUES
Initial learning rate for SGD optimization.	Range(0.00001, 0.001)
SGD full passes to dataset (epochs).	DiscreteRange(25, 3000)
Random seed that controls initialization of weights.	DiscreteRange(1, 10)
SGD Batch Size.	DiscreteRange(4, 100)
Activation Function.	PeLU
Temporal Convolution Kernel Size.	$N_{ck} \in \{2, 7\}$
Temporal Convolution Layers.	$N_{cl} \in \{3, 5\}$
Temporal Convolution Filters.	$N_{cf} \in \{10, 30\}$
Future Encoder Dimension.	$N_f \in \{50\}$
Static Encoder Dimension.	$N_s \in \{100\}$
Horizon Agnostic Decoder Dimensions.	$N_{ag} \in \{50\}$
Horizon Specific Decoder Dimensions.	$N_{sp} \in \{20\}$
Poisson Mixture Weights Decoder Layers.	$N_{wdl} \in \{3, 4\}$
Poisson Mixture Rate Decoder Layers.	$N_{rdl} \in \{2, 3, 4\}$
Local Decoder Dimensions.	$N_k \in \{25, 50, 100\}$

## 6.2. Evaluation Metrics

The evaluation of the model’s predictions is based on the *quantile loss* (QL) (Matheson & Winkler, 1976); consider the estimated cumulative distribution function  $\hat{\mathbf{F}}_{i,\tau}$  for an observation  $y_{i,\tau}$ , the loss is defined as:

$$\text{QL}(\hat{\mathbf{F}}_{i,\tau}, y_{i,\tau})_q = 2 \left( \mathbb{1}\{y_{i,\tau} \leq \hat{\mathbf{F}}_{i,\tau}^{-1}(q)\} - q \right) \left( \hat{\mathbf{F}}_{i,\tau}^{-1}(q) - y_{i,\tau} \right) \quad (20)$$

We summarize the evaluation, for convenience of exposition and to ensure the comparability of our results with the existing literature, using the *continuous ranked probability score*, abbreviated as CRPS (Matheson & Winkler, 1976). The CRPS measures the accuracy of the predictive distributions and has desirable theoretical properties as a metric (Gneiting & Ranjan, 2011). Following notation from Laio & Tamea 2007, the CRPS<sup>5</sup> is defined as:

$$\text{CRPS}(\hat{\mathbf{F}}_{i,\tau}, y_{i,\tau}) = \int_0^1 \text{QL}(\hat{\mathbf{F}}_{i,\tau}, y_{i,\tau})_q dq \quad (21)$$

## 6.3. Training Methodology and Hyperparameter Optimization

As shown in Table 2, the hyperparameter space that we consider for optimization is minimal. We only tune the learning rate, random seed to escape underperforming local minima, and the number of SGD epochs as a form of regularization (Yao et al., 2007). During the *hyperparameter optimization phase*, we measure the model CRPS performance on the validation set described in Section 6.1, and use HYPEROPT (Bergstra et al., 2011), a Bayesian optimization library, to efficiently explore the hyperparameters based on the validation measurements.

<sup>5</sup>In practice the evaluation of the CRPS uses numerical integration technique, that discretizes the quantiles and treats the integral with a left Riemann approximation, averaging over uniformly distanced quantiles.



Table 3: Empirical evaluation of probabilistic, hierarchical forecasts. Mean *continuous ranked probability score* (CRPS) for predictions, averaged over 8 runs, at each aggregation level, the best result is highlighted (lower is better). The mean hierarchical methods have unique solutions, and constant results over the runs.

\* The ARIMA-ERM results for Tourism-L differ from Rangapuram et al. (2021), as we improved the numerical stability of their implementation.

\*\* PERMBU-MinT on Tourism-L is unavailable because the original implementation can't be applied to grouping structures with more than a single hierarchy.

DATASET	LEVEL	DPMN-GroupBU (prob.)	DPMN-NaiveBU (prob.)	HierE2E (prob.)	PERMBU-MinT** (prob.)	ERM* (mean)	MinT-shr (mean)	NaiveBU (mean)
Traffic	Overall	0.0548 ± 0.0102	<b>0.0350 ± 0.0007</b>	0.0376 ± 0.0060	0.0677 ± 0.0061	0.0466	0.077	0.0753
	1 (geo.)	0.0357 ± 0.0139	<b>0.0064 ± 0.0010</b>	0.0184 ± 0.0091	0.0331 ± 0.0085	0.0087	0.045	0.0363
	2 (geo.)	0.0371 ± 0.0127	0.0142 ± 0.0008	0.0181 ± 0.0086	0.0341 ± 0.0081	<b>0.0112</b>	0.046	0.0363
	3 (geo.)	0.0368 ± 0.0120	<b>0.0144 ± 0.0007</b>	0.0223 ± 0.0072	0.0417 ± 0.0061	0.0255	0.046	0.0453
	4 (geo.)	0.1094 ± 0.0050	0.1049 ± 0.0004	<b>0.0914 ± 0.0024</b>	0.1621 ± 0.0027	0.1410	0.1701	0.1832
Tourism-L	Overall	<b>0.1260 ± 0.0046</b>	0.1578 ± 0.0084	0.1520 ± 0.0032	-	0.1689	0.1609	0.1741
	1 (geo.)	<b>0.0411 ± 0.0110</b>	0.1130 ± 0.0197	0.0810 ± 0.0053	-	0.0725	0.0438	0.0827
	2 (geo.)	<b>0.0624 ± 0.0070</b>	0.1189 ± 0.0161	0.1030 ± 0.0030	-	0.1071	0.0816	0.1035
	3 (geo.)	<b>0.1122 ± 0.0049</b>	0.1466 ± 0.0131	0.1361 ± 0.0024	-	0.1541	0.1433	0.1586
	4 (geo.)	<b>0.1571 ± 0.0032</b>	0.1759 ± 0.0125	0.1752 ± 0.0026	-	0.2052	0.2036	0.2131
	5 (prp.)	<b>0.0747 ± 0.0056</b>	0.1315 ± 0.0060	0.1027 ± 0.0062	-	0.1095	0.0830	0.1002
	6 (prp.)	<b>0.1100 ± 0.0044</b>	0.1416 ± 0.0058	0.1403 ± 0.0047	-	0.1628	0.1479	0.1567
	7 (prp.)	<b>0.1901 ± 0.0046</b>	0.1908 ± 0.0052	0.2050 ± 0.0028	-	0.2435	0.2437	0.2489
	8 (prp.)	0.2600 ± 0.0039	<b>0.2428 ± 0.0045</b>	0.2727 ± 0.0017	-	0.3076	0.3406	0.3379
Favorita	Overall	<b>0.1975 ± 0.0060</b>	0.2653 ± 0.0063	0.2698 ± 0.0031	0.2335 ± 0.0024	0.3675	0.2606	0.2652
	1 (geo.)	0.1365 ± 0.0082	0.2080 ± 0.0109	0.2396 ± 0.0034	<b>0.1346 ± 0.0019</b>	0.2979	0.1468	0.1556
	2 (geo.)	<b>0.1892 ± 0.0065</b>	0.2568 ± 0.0056	0.2664 ± 0.0031	0.1912 ± 0.0023	0.3593	0.2176	0.2176
	3 (geo.)	<b>0.1994 ± 0.0061</b>	0.2663 ± 0.0058	0.2738 ± 0.0039	0.3419 ± 0.0027	0.3729	0.3769	0.3769
	4 (geo.)	<b>0.2649 ± 0.0040</b>	0.3299 ± 0.0079	0.3086 ± 0.0034	0.2766 ± 0.0029	0.4408	0.3096	0.3132

After the optimal hyperparameters are determined, we estimate the model parameters again by shifting the training window forward, noted as the *retrain phase*, and predict for the final test set. We refer to the combination of the *hyperparameter optimization* and *retrain* phases as a *run*. The DPMN is implemented using MXNet (Tianqi Chen et al., 2015). To train the network, we minimize the negative log-likelihood of the corresponding composite likelihood variant from Section 4, using stochastic gradient descent<sup>6</sup> with *Adaptive Moments* (ADAM; Kingma & Ba 2014).

#### 6.4. Forecasting Results

We compare against the predictions of the following hierarchical methods across the hierarchical levels: (1) HierE2E (Rangapuram et al., 2021) that combines a deep vector autoregressive approach with hierarchical constraints<sup>7</sup>, (2) PERMBU-MinT<sup>8</sup> (Taieb et al., 2017) that performs a probabilistic hierarchical aggregation that reconciles unbiased independent forecasts and minimizes the bias-variance trade-off of the errors. Additionally, we report the evaluation of the following mean hierarchical methods: (3) ERM (Ben Taieb & Koo, 2019) that performs an optimization-based reconciliation free of the unbiasedness assumption of the base forecasts, (4) MinT<sup>9</sup> (Wickramasuriya et al., 2019) meant to reconcile unbiased independent forecasts and minimize the variance of the forecast errors, and (5) NaiveBU (Orcutt et al., 1968) that produces univariate bottom-level time-series predictions

<sup>6</sup>We modified the stochastic gradient descent to sample at the composite likelihood group level.

<sup>7</sup>The HierE2E benchmark models and experiments are available in a [GluonTS library](#) extension.

<sup>8</sup>The original PERMBU-MinT is implemented in [supplementary material](#) of the work of Taieb et al. (2017)

<sup>9</sup>The original implementation of MinT is available in the R package `hts` (Hyndman et al., 2020), it automatically selects ARIMA univariate base forecast methods (Hyndman & Khandakar, 2008).

independently and then sums them according to the hierarchical constraints. The last three methods in their original form produce point predictions. Thus, we evaluate the CRPS treating the predictions as a degenerate distributional forecast with collapsed support in the mean. This proof of concept sets expectations on the probabilistic algorithms’ accuracy.

For our proposed methods, we report the **DPMN-NaiveBU** and the **DPMN-GroupBU**. As described in Section 4, the **DPMN-NaiveBU** treats the bottom level series as independent observations, and the **DPMN-GroupBU** considers groups of time series during its composite likelihood estimation. Both methods obtain probabilistic coherent predictions using the bottom-up reconciliation. The comparison of the DPMN variants serves as an ablation experiment to better analyze the source of the accuracy improvements. It also showcases the ability of the Poisson Mixture model to give good results for unseen hierarchical structures, and in the case of the **Traffic** dataset, of uninformative or noisy time-series group structure, to explore the limits of the **GroupBU** estimation method.

Table 3 contains the CRPS measurements for the predictive distributions at each aggregation level through the whole dataset hierarchy. The top row reports the overall CRPS score (averaged across all the hierarchy levels). We highlight the best result in **bolds**.

The DPMN significantly and consistently improves the overall CRPS for **Tourism-L** and **Favorita**. In particular, the **DPMN-GroupBU** variant shows improvements of 17.1% percent against the second-best alternative in the **Tourism-L** dataset and 24.2% percent against the second-best choice in the **Favorita** dataset. In the **Traffic** dataset, the **DPMN-GroupBU** variant does not benefit from modeling the uninformative correlations between highways, and subsequently does not improve upon the other compared methods. The **DPMN-NaiveBU** variant performs well on **Traffic** relative to the benchmarks, and gives an acceptable performance on **Tourism-L** and **Favorita** compared to that of well performing statistical alternatives.

Our results confirm observations from the community that a shared model, capable of learning from all the time series jointly, improves the predictions over those from univariate time series methods. Additionally, the qualitative comparison<sup>10</sup> between the **NaiveBU** and **GroupBU** methods shows that an expressive joint distribution framework capable of leveraging the hierarchical structure of the data, when informative, is beneficial for the accuracy of the predictions. For **Traffic** data where the aggregate time series have narrow predictive distributions, **NaiveBU** is more suitable than **GroupBU**, because when predictive distributions are degenerate, the value of predicting accurate bottom-level time series exceeds that of learning correlations between time series.

## 7. Conclusions and Future Work

In this work, we have introduced a novel method for probabilistic hierarchical forecasting, the *Deep Poisson Mixture Network* (DPMN), which focuses on learning the joint distribution of bottom level time series and naturally guarantees hierarchical coherence. We have

---

<sup>10</sup>Figure A.1 and Figure A.2 in the Appendix show a qualitative exploration of the **NaiveBU** and **GroupBU** versions of the DPMN model.

also shown through empirical evaluations that our model is accurate for count data. We observed overall significant improvements in CRPS when compared with previous state-of-the-art probabilistically coherent models on three different hierarchical datasets, Australian domestic tourism (17.1%), Ecuadorian grocery sales (24.2%), and San Francisco Bay Area traffic data (6.9%).

The framework presented here is also extensible. We chose to focus on forecasting count data and used Poisson kernels, but one could also use Gaussian kernels to model joint distributions of real valued hierarchical data. In fact, any kernel which admits closed form expression for aggregated distributions under conditional independence akin to Eq. 5 will work well, and it includes kernels like the Gamma and the Negative Binomial distributions in addition to the Poisson and the Gaussian distributions already mentioned. By formulating the model as a Mixture Density Network, we have separated the probabilistic model of the predictive distribution from the underlying neural architecture. In the current paper we relied on the convolutional encoder version of the `MQ-Forecaster` architecture, but significant progress has been made in the last few years on neural network based forecasting models; for example, Transformer-based deep learning architectures (Eisenach et al., 2021) that can improve performance. We plan to explore both directions, new kernels and new neural network architectures in future work.

DPMN has its drawbacks as well. As is the case with any finite mixture model, the fidelity of the estimated distribution depends on the number of mixture components. A few hundred samples may be sufficient to describe a single marginal distribution but can be too sparse to describe the joint distribution in a high dimensional space. The sparsity will be particularly obvious if customers of hierarchical forecasting are interested in forecast distributions conditioned on partially observed data. The small number of samples will lead to overly confident posterior distributions. Another issue is the model misspecification during inference. The component matching method performs quite well in empirical evaluations but is somewhat unsatisfactory as a statistical model. To mitigate both issues we are exploring generative factor models where the mixture components are truly samples from an underlying distribution and correlations between marginal distributions will be captured by common factors. It will bring DPMN closer to standard Hierarchical Bayesian formulation but with fewer and less strict assumptions.

## Acknowledgements

Thanks to Dr. Kari Torkkola and Dr. Michael Mahoney for in-depth suggestions and discussion on the presentation and the experiment design. Thanks to all Amazon Forecasting Science team members for their comments and feedback on literature review and writing. Thanks to Stefania La Vattiata for her assistance in the upbeat exposition of the *Deep Poisson Mixture Network*. The authors are also grateful to Syama Rangapuram and Pedro Mercado that carefully chose and organized hierarchical forecasting baselines. And Federico Garza for his help in the replication of the baselines.

## References

- Athanasopoulos, G., Hyndman, R. J., Kourentzes, N., & Petropoulos, F. (2017). Forecasting with temporal hierarchies. *European Journal of Operational Research*, 262, 60–74.
- Atiya, A., & Taieb, B. (2016). A bias and variance analysis for multistep-ahead time series forecasting. *IEEE transactions on neural networks and learning systems*, 27, 2162–2388. URL: <https://pubmed.ncbi.nlm.nih.gov/25807572/>.
- Ben Taieb, S., & Koo, B. (2019). Regularized regression for hierarchical forecasting without unbiasedness conditions. In *Proceedings of the 25th ACM SIGKDD International Conference on Knowledge Discovery & Data Mining KDD '19* (p. 1337–1347). New York, NY, USA: Association for Computing Machinery. URL: <https://doi.org/10.1145/3292500.3330976>. doi:10.1145/3292500.3330976.
- Bergstra, J., Bardenet, R., Bengio, Y., & Kégl, B. (2011). Algorithms for hyper-parameter optimization. In J. Shawe-Taylor, R. Zemel, P. Bartlett, F. Pereira, & K. Q. Weinberger (Eds.), *Advances in Neural Information Processing Systems* (pp. 2546–2554). Curran Associates, Inc. volume 24. URL: <https://proceedings.neurips.cc/paper/2011/file/86e8f7ab32cfd12577bc2619bc635690-Paper.pdf>.
- Bishop, C. M. (1994). *Mixture density networks*. Technical Report Aston University Birmingham. URL: <https://publications.aston.ac.uk/id/eprint/373/>.
- Böse, J.-H., Flunkert, V., Gasthaus, J., Januschowski, T., Lange, D., Salinas, D., Schelter, S., Seeger, M., & Wang, Y. (2017). Probabilistic demand forecasting at scale. *Proc. VLDB Endow.*, 10, 1694–1705. URL: <https://doi.org/10.14778/3137765.3137775>. doi:10.14778/3137765.3137775.
- Cho, K., van Merriënboer, B., Gülçehre, Ç., Bougares, F., Schwenk, H., & Bengio, Y. (2014). Learning phrase representations using RNN encoder-decoder for statistical machine translation. *Proceedings of the 2014 Conference on Empirical Methods in Natural Language Processing (EMNLP)*, abs/1406.1078, 1724–1734. URL: <http://arxiv.org/abs/1406.1078>. arXiv:1406.1078.
- Christiansen, C. L., & Morris, C. N. (1997). Hierarchical poisson regression modeling. *Journal of the American Statistical Association*, 92, 618–632.
- Corporación Favorita (2018). Corporación favorita grocery sales forecasting. Kaggle Competition. URL: <https://www.kaggle.com/c/favorita-grocery-sales-forecasting/>.
- Diggle, P., & Brix, A. (2001). Spatio-temporal prediction for log-gaussian cox processes. *Journal of the Royal Statistical Society: Series B (Statistical Methodology)*, 63, 823–841. doi:10.1111/1467-9868.00315.
- Diggle, P. J. (2013). *Statistical Analysis of Spatial and Spatio-Temporal Point Patterns*. (Third edition ed.). Routledge.
- Dua, D., & Graff, C. (2017). UCI machine learning repository. URL: <http://archive.ics.uci.edu/ml>.
- Eisenach, C., Patel, Y., & Madeka, D. (2021). MQTransformer: Multi-Horizon Forecasts with Context Dependent and Feedback-Aware Attention. In M. F. Balcan, & M. Meila (Eds.), *Submitted to Proceedings of the 38th International Conference on Machine Learning*. PMLR. Working Paper version available at arXiv:2009.14799.
- Flidner, G. (1999). An investigation of aggregate variable time series forecast strategies with specific subaggregate time series statistical correlation. *Computers and Operations Research*, 26, 1133–1149. URL: [https://doi.org/10.1016/S0305-0548\(99\)00017-9](https://doi.org/10.1016/S0305-0548(99)00017-9). doi:10.1016/S0305-0548(99)00017-9.
- Fotios Petropoulos et. al. (2021). Forecasting: theory and practice. arXiv:2012.03854.
- Gneiting, T., & Katzfuss, M. (2014). Probabilistic forecasting. *Annual Review of Statistics and Its Application*, 1, 125–151. URL: <https://ssrn.com/abstract=2405902>.
- Gneiting, T., & Ranjan, R. (2011). Comparing density forecasts using threshold-and quantile-weighted scoring rules. *Journal of Business & Economic Statistics*, 29, 411–422.
- Gross, C. W., & Sohl, J. E. (1990). Disaggregation methods to expedite product line forecasting. *Journal of Forecasting*, 9, 233–254. URL: <https://onlinelibrary.wiley.com/doi/abs/10.1002/for.3980090304>. doi:10.1002/for.3980090304.
- Han, X., Dasgupta, S., & Ghosh, J. (2021). Simultaneously reconciled quantile forecasting of hierarchically related time series. In A. Banerjee, & K. Fukumizu (Eds.), *Proceedings of The 24th International Conference on Artificial Intelligence and Statistics* (pp. 190–198). PMLR volume 130 of *Proceedings of Machine Learning Research*. URL: <http://proceedings.mlr.press/v130/han21a.html>.

- Hollyman, R., Petropoulos, F., & Tipping, M. E. (2021). Understanding forecast reconciliation. *European Journal of Operational Research*, *294*, 149–160. URL: <https://www.sciencedirect.com/science/article/pii/S0377221721000199>. doi:<https://doi.org/10.1016/j.ejor.2021.01.017>.
- Hong, T., Pinson, P., & Fan, S. (2014). Global energy forecasting competition 2012.
- Hyndman, R. J., Ahmed, R. A., Athanasopoulos, G., & Shang, H. L. (2011). Optimal combination forecasts for hierarchical time series. *Computational Statistics & Data Analysis*, *55*, 2579 – 2589. URL: <http://www.sciencedirect.com/science/article/pii/S0167947311000971>. doi:<https://doi.org/10.1016/j.csda.2011.03.006>.
- Hyndman, R. J., & Athanasopoulos, G. (2018). *Forecasting: Principles and Practice*. Melbourne, Australia: OTexts. Available at <https://otexts.com/fpp2/>.
- Hyndman, R. J., & Khandakar, Y. (2008). Automatic time series forecasting: The forecast package for r. *Journal of Statistical Software, Articles*, *27*, 1–22. URL: <https://www.jstatsoft.org/v027/i03>. doi:10.18637/jss.v027.i03.
- Hyndman, R. J., Lee, A., & Wang, E. (2014). *Fast computation of reconciled forecasts for hierarchical and grouped time series*. Monash Econometrics and Business Statistics Working Papers 17/14 Monash University, Department of Econometrics and Business Statistics. URL: <https://ideas.repec.org/p/msh/ebswps/2014-17.html>.
- Hyndman, R. J., Lee, A., Wang, E., Wickramasuriya, S., & Wang, M. E. (2020). *Package hts: Hierarchical and Grouped Time Series*. URL: <https://CRAN.R-project.org/package=hts>. R package version 6.0.1.
- Jeon, J., Panagiotelis, A., & Petropoulos, F. (2019). Probabilistic forecast reconciliation with applications to wind power and electric load. *European Journal of Operational Research*, *279*, 364–379.
- Kingma, D. P., & Ba, J. (2014). ADAM: A method for stochastic optimization. URL: <http://arxiv.org/abs/1412.6980> cite arxiv:1412.6980Comment: Published as a conference paper at the 3rd International Conference for Learning Representations (ICLR), San Diego, 2015.
- Laio, F., & Tamea, S. (2007). Verification tools for probabilistic forecasts of continuous hydrological variables. *Hydrology and Earth System Sciences*, *11*, 1267–1277.
- Lindsay, B. G. (1988). Composite likelihood methods. *Contemporary Mathematics*, *80*, 221–239.
- Madeka, D., Swiniarski, L., Foster, D., Razoumov, L., Torkkola, K., & Wen, R. (2018). Sample path generation for probabilistic demand forecasting. In *ICML workshop on Theoretical Foundations and Applications of Deep Generative Models*.
- Makridakis, S., Spiliotis, E., & Assimakopoulos, V. (2018). The M4 competition: Results, findings, conclusion and way forward. *International Journal of Forecasting*, *34*, 802 – 808. URL: <http://www.sciencedirect.com/science/article/pii/S0169207018300785>. doi:<https://doi.org/10.1016/j.ijforecast.2018.06.001>.
- Makridakis, S., Spiliotis, E., & Assimakopoulos, V. (2020). The M5 accuracy competition: Results, findings and conclusions. *International Journal of Forecasting*, . URL: [https://www.researchgate.net/publication/344487258\\_The\\_M5\\_Accuracy\\_competition\\_Results\\_findings\\_and\\_conclusions](https://www.researchgate.net/publication/344487258_The_M5_Accuracy_competition_Results_findings_and_conclusions).
- Matheson, J. E., & Winkler, R. L. (1976). Scoring rules for continuous probability distributions. *Management Science*, *22*, 1087–1096. URL: <http://www.jstor.org/stable/2629907>.
- Olivares, K. G., Challu, C., Marcjasz, G., Weron, R., & Dubrawski, A. (2021). Neural basis expansion analysis with exogenous variables: Forecasting electricity prices with NBEATSx. *International Journal of Forecasting, submitted, Working Paper version available at arXiv:2104.05522*.
- van den Oord, A., Dieleman, S., Zen, H., Simonyan, K., Vinyals, O., Graves, A., Kalchbrenner, N., Senior, A. W., & Kavukcuoglu, K. (2016). WaveNet: A generative model for raw audio. *Computer Research Repository, abs/1609.03499*. URL: <http://arxiv.org/abs/1609.03499>. arXiv:1609.03499.
- Orcutt, G. H., Watts, H. W., & Edwards, J. B. (1968). Data aggregation and information loss. *The American Economic Review*, *58*, 773–787. URL: <http://www.jstor.org/stable/1815532>.
- Panagiotelis, A., Gamakumara, P., Athanasopoulos, G., & Hyndman, R. J. (2020). *Probabilistic Forecast Reconciliation: Properties, Evaluation and Score Optimisation*. Monash Econometrics and Business Statistics Working Papers 26/20 Monash University, Department of Econometrics and Business Statistics. URL: <https://ideas.repec.org/p/msh/ebswps/2020-26.html>.

- Paria, B., Sen, R., Ahmed, A., & Das, A. (2021). Hierarchically Regularized Deep Forecasting. In *Submitted to Proceedings of the 39th International Conference on Machine Learning*. PMLR. Working Paper version available at arXiv:2106.07630.
- Park, B.-J., & Lord, D. (2009). Application of finite mixture models for vehicle crash data analysis. *Accident Analysis & Prevention*, *41*, 683–691.
- Puwasala, G., Panagiotelis Anastasios, G., Athanasopoulos, & Hyndman, R. J. (2018). Probabilistic Forecasts in Hierarchical Time Series. *Department of Econometrics and Business Statistics Working Paper Series 11/18*, .
- Rangapuram, S. S., Werner, L. D., Benidis, K., Mercado, P., Gasthaus, J., & Januschowski, T. (2021). End-to-end learning of coherent probabilistic forecasts for hierarchical time series. In M. F. Balcan, & M. Meila (Eds.), *Proceedings of the 38th International Conference on Machine Learning* Proceedings of Machine Learning Research. PMLR.
- Ravuri, S. V., Lenc, K., Willson, M., Kangin, D., Lam, R., Mirowski, P., Fitzsimons, M., Athanassiadou, M., Kashem, S., Madge, S., Prudden, R., Mandhane, A., Clark, A., Brock, A., Simonyan, K., Hadsell, R., Robinson, N. H., Clancy, E., Arribas, A., & Mohamed, S. (2021). Skillful precipitation nowcasting using deep generative models of radar. *Nature*, *597*, 672–691. URL: <https://www.nature.com/articles/s41586-021-03854-z.pdf>.
- Rosenblatt, F. (1961). *Principles of neurodynamics. perceptrons and the theory of brain mechanisms*. Technical Report Cornell Aeronautical Lab Inc Buffalo NY.
- Spiliotis, E., Petropoulos, F., Kourntzes, N., & Assimakopoulos, V. (2020). Cross-temporal aggregation: Improving the forecast accuracy of hierarchical electricity consumption. *Applied Energy*, *261*, 114339.
- Taieb, S. B., Taylor, J. W., & Hyndman, R. J. (2017). Coherent probabilistic forecasts for hierarchical time series. In D. Precup, & Y. W. Teh (Eds.), *Proceedings of the 34th International Conference on Machine Learning* (pp. 3348–3357). PMLR volume 70 of *Proceedings of Machine Learning Research*. URL: <http://proceedings.mlr.press/v70/taieb17a.html>.
- Tianqi Chen et al. (2015). Mxnet: A flexible and efficient machine learning library for heterogeneous distributed systems. *CoRR*, *abs/1512.01274*. URL: <http://arxiv.org/abs/1512.01274>.
- Tourism Australia, Canberra (2019). Detailed tourism Research Australia (2005), Travel by Australians. Accessed at <https://robjhyndman.com/publications/hierarchical-tourism/>.
- Van Erven, T., & Cugliari, J. (2015). Game-theoretically optimal reconciliation of contemporaneous hierarchical time series forecasts. In *Modeling and stochastic learning for forecasting in high dimensions* (pp. 297–317). Springer.
- Varin, C., Reid, N., & Firth, D. (2011). An overview of composite likelihood methods. *Statistica Sinica*, *21*, 5–42. URL: <http://www.jstor.org/stable/24309261>.
- Wen, R., Torkkola, K., Narayanaswamy, B., & Madeka, D. (2017). A Multi-horizon Quantile Recurrent Forecaster. In *31st Conference on Neural Information Processing Systems NIPS 2017, Time Series Workshop*. URL: <https://arxiv.org/abs/1711.11053>. arXiv:1711.11053.
- Wickramasuriya, S. L., Athanasopoulos, G., & Hyndman, R. J. (2019). Optimal forecast reconciliation for hierarchical and grouped time series through trace minimization. *Journal of the American Statistical Association*, *114*, 804–819. URL: <https://robjhyndman.com/publications/mint/>. doi:10.1080/01621459.2018.1448825.
- Wikle, C. K., Berliner, L. M., & Cressie, N. (1998). Hierarchical bayesian space-time models. *Environmental and ecological statistics*, *5*, 117–154.
- Yao, Y., Rosasco, L., & Andrea, C. (2007). On early stopping in gradient descent learning. *Constructive Approximation*, *26(2)*, 289–315. URL: <https://doi.org/10.1007/s00365-006-0663-2>.
- Yu, B., Yin, H., & Zhu, Z. (2018). Spatio-temporal graph convolutional neural network: A deep learning framework for traffic forecasting. In *Proceedings of the 27th International Joint Conference on Artificial Intelligence (IJCAI)*. URL: <http://arxiv.org/abs/1709.04875>.

## Appendix A. Appendix

### Appendix A.1. Dataset Details

The **Traffic** dataset, as mentioned, measures the occupancy rates of 963 freeway lanes from the Bay Area. The original data is at a 10-minute frequency from January 1st 2008 to March 30th 2009. The dataset is further aggregated from the 10-minute frequency into daily frequency with 366 observations. We match the sample procedure from previous hierarchical forecasting literature (Ben Taieb & Koo, 2019; Rangapuram et al., 2021), and use the same 200 bottom level series from the 963 available. From these 200 bottom level series a hierarchy is randomly defined by aggregating them into quarters and halves of 50 and 100 series each, finally we consider the total aggregation. Table A1 describes the hierarchical structure.

Table A1: San Francisco Bay Area Highway Traffic.  
\* The hierarchical structure is randomly defined.

Geographical Level *	Series per Level
Bay Area	1
Halves	2
Quarters	4
Bottom	200
Total	207

The **Tourism-L** dataset contains 555 monthly series from 1998 to 2016, it is organized by geography and purpose of travel. The four-level geographical hierarchy comprises seven states, divided further into 27 zones and 76 regions. The categories for purpose of travel are holiday, visiting friends and relatives, business and other. This dataset has been referenced by important hierarchical forecasting studies like the one of the **MinT** reconciliation strategy and the more recent **HierE2E** (Wickramasuriya et al., 2019; Rangapuram et al., 2021). **Tourism-L** is a grouped dataset, it has two dimensions in which it is aggregated, the total level aggregation and its four associated purposes. Table A2 describes the group and hierarchical structures.

Table A2: Australian Tourism flows.

Geographical Level	Series per Level	Series per Level & Purpose	Total
Australia	1	4	5
States	7	28	35
Zones	27	108	135
Regions	76	304	380
Total	111	444	555

The **Favorita** dataset, once balanced for items and stores, contains 217,944 bottom level series, in contrast the original competition considers 210,645 series. We resort for this balance because, for the moment the **GroupBU** version of the **PMM** requires balanced hierarchies for its estimation. In the case of the **Favorita** experiment we consider a geographical hierarchy (93 nodes) conditional of each of grocery item (4,036). The hierarchy defines 153,368 new aggregate series at the item-country, item-state, and item-city levels. Table A3 describes the structure. Regarding the dataset preprocessing, we confirmed observations from the best submissions to the Kaggle competition. Most holiday distances included in the dataset and covariates like oil production lack value for the predictions. The models did not benefit from a long history, filtering the training window to the 2017 year consistently produced better results.

Table A3: Favorita Grocery Sales.

<b>Geographical Level</b>	<b>Nodes per Level</b>	<b>Series per Level</b>	<b>Total</b>
Ecuador	1	4,036	4,036
States	16	64,576	64,576
Cities	22	88,792	88,792
Stores	54	217,944	217,944
<b>Total</b>	<b>93</b>	<b>371,312</b>	<b>371,312</b>



## Appendix A.2. Model Parameter Details

Table A4: *Deep Poisson Mixture Network* (DPMN) architecture parameters configured once per dataset. These hyperparameters were not considered during the hyperparameter optimization phase.

PARAMETER	Notation	Considered Values		
		TOURISM-L	FAVORITA	TRAFFIC
SGD Batch Size.	-	4	100	4
Activation Function.	-	PeLU	PeLU	PeLU
Temporal Convolution Kernel Size.	$N_{ck}$	{2}	{2}	{7}
Temporal Convolution Layers.	$N_{cl}$	{5}	{5}	{3}
Temporal Convolution Filters.	$N_p$	{30}	{30}	{10}
Future Encoder Dimension.	$N_f$	{50}	{50}	{50}
Static Encoder Dimension.	$N_s$	{100}	{100}	{100}
Horizon Agnostic Decoder Dimensions.	$N_{ag}$	{50}	{50}	{50}
Horizon Specific Decoder Dimensions.	$N_{sp}$	{20}	{20}	{20}
Poisson Mixture Weight Decoder Layers.	$N_{wdl}$	{4}	{4}	{3}
Poisson Mixture Rate Decoder Layers.	$N_{rdl}$	{3}	{3}	{2}
Poisson Mixture Components.	$N_k$	{100}	{100}	{25}
GPU Training Configuration.	-	2 x NVIDIA K80	4 x NVIDIA V100	2 x NVIDIA V100

As mentioned in Section 6.3, the hyperparameter space is minimal, as we only consider for the optimization the learning rate, random initialization of the weights, and SGD epochs. Regarding the batch size, we found for **Favorita** and **Tourism-L** that maximizing its value with respect to GPU memory limitations resulted in the optimal performance; for **Traffic**, though the entire dataset could fit in memory at once, it was preferable to feed in subsets to allow the model to learn from different groupings of highways in each epoch. Regarding the architecture parameters, we relied on domain expertise for its selection. In particular, since **Traffic** is the smallest dataset, we opted for a reduced model size and number of Poisson mixture components, to control the model’s variability. Additionally due to the strong weekly seasonality pattern in the dataset, we also adjusted the temporal convolution kernel size to encompass seven days.

Appendix A.3. Deep Poisson Mixture Network predictions comparison

Appendix A.3.1. DPMN Naive Bottom Up predictions

As mentioned in Section 4, composite likelihood may suffer from model misspecification. The DPMN-NaiveBU does not learn the dependencies or correlations between time-series in the hierarchy. As shown in Figure A.1 the DPMN-NaiveBU produces prediction distributions for the aggregate levels unnecessarily wide, as it pushes the limits of the aggregation rule.

Still, the DPMN-NaiveBU performs well in disaggregated series and means as we show in the empirical evaluation of Section 6. The DPMN-NaiveBU produces predictions comparable to those of statistical alternatives on the **Tourism-L** and **Favorita** datasets and outperforms all the other algorithms in the **Traffic** dataset where the hierarchical structure is noisy or not as informative.

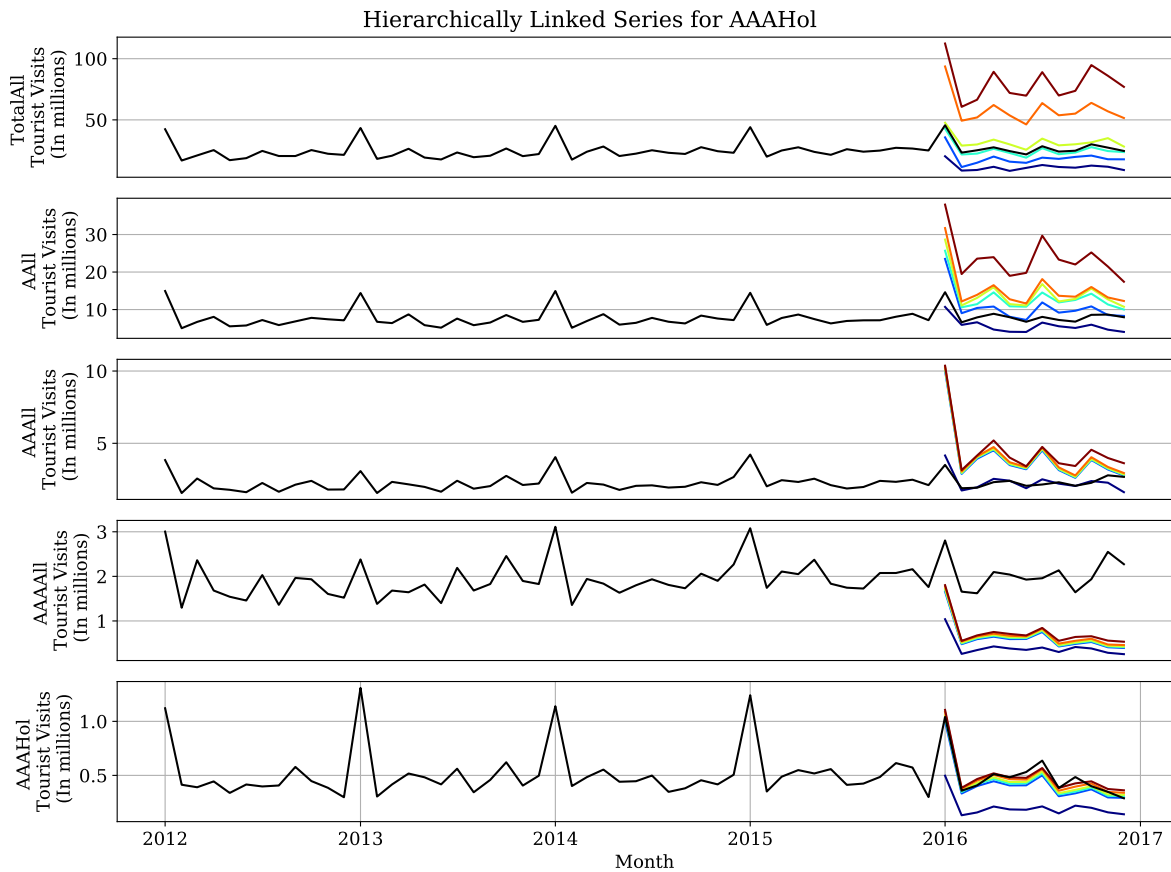


Figure A.1: DPMN-NaiveBU predictive distributions on a hierarchically linked time series from the **Tourism-L** dataset. The top row shows the total number of tourist visits in Australia (**TotalAll**), the second row shows the visits to Australia for the North South Wales state (**AAll**), the third row shows the holiday visits in the metropolitan Area of New South Wales (**AAAll**), the fourth row shows the holiday visits in Sidney (**AAAAAll**), the final row shows the holiday visits to Sidney. Quantile predictions are shown in colored lines.

### Appendix A.3.2. DPMN Group Bottom Up predictions

The **GroupBU** composite likelihood estimation method considers dependencies and correlations between time series. When in the presence of informative time-series group structures, the **DPMN-GroupBU** uses the expressiveness of the multivariate Poisson joint distribution to its advantage. It better models the dependencies within the time-series groups it considers during its estimation while remaining computationally tractable.

As we show in Section 6 and Figure A.2 when in the presence of strong correlation structures between the time series, like the ones in the **Tourism-L** and **Favorita** datasets, the **DPMN-GroupBU** outperforms all the hierarchical forecasting alternatives that we considered in our experiments. However, we showcase the limits of the method when the groups of series considered by the model are noisy or as informative as the case of the **Traffic** dataset where the group structure was randomly assigned.

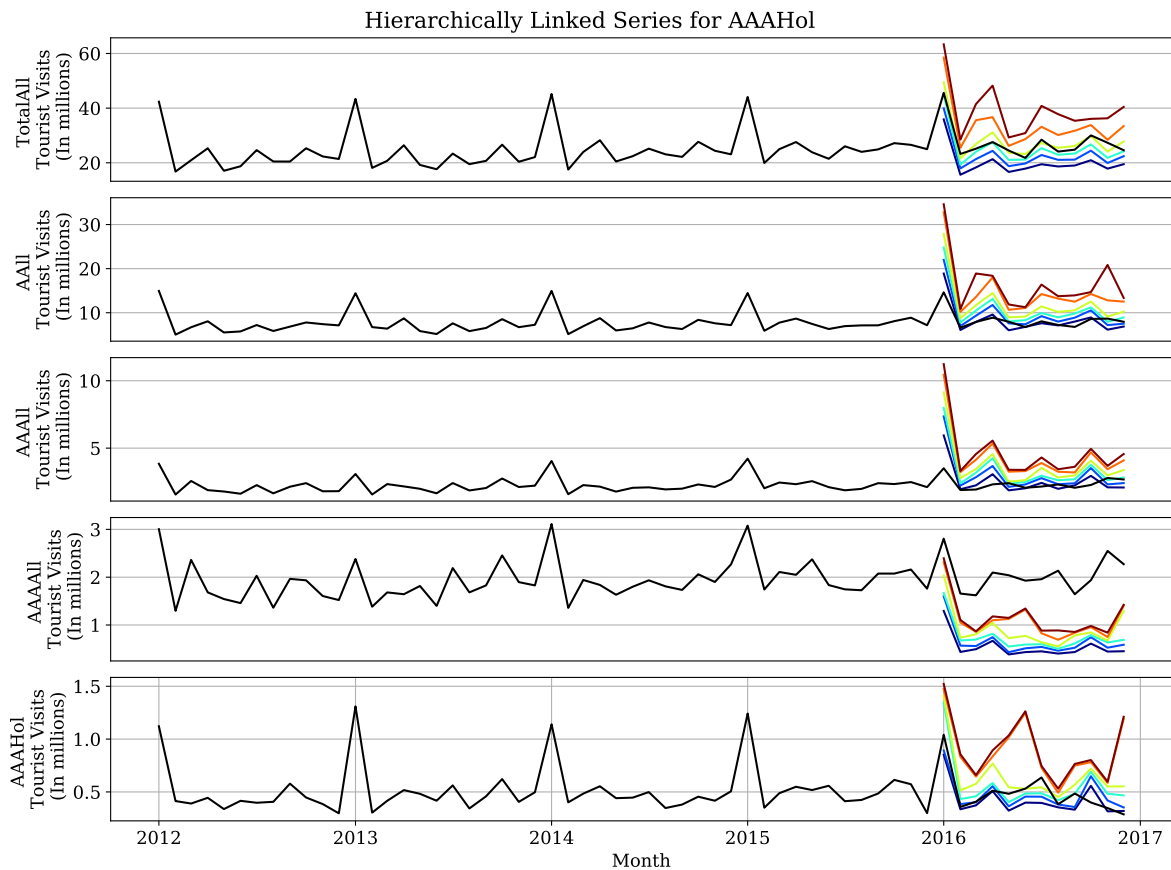


Figure A.2: **DPMN-GroupBU** predictive distributions on a hierarchically linked time series from the **Tourism-L** dataset. The top row shows the total number of tourist visits in Australia (**TotalAll**), the second row shows the visits to Australia for the North South Wales state (**AAll**), the third row shows the holiday visits in the metropolitan Area of New South Wales (**AAAll**), the fourth row shows the holiday visits in Sidney (**AAAAll**), the final row shows the holiday visits to Sidney. Quantile predictions are shown in colored lines.